

RESEARCH ARTICLE

Uptake in non-affected bone tissue does not differ between [¹⁸F]-DCFPyL and [⁶⁸Ga]-HBED-CC PSMA PET/CT

Jochen Hammes^{1*}, Melanie Hohberg¹, Philipp Täger¹, Markus Wild¹, Boris Zlatopolskiy², Philipp Krapf³, Bernd Neumaier^{2,3}, Klaus Schomäcker¹, Carsten Kobe¹, Matthias Schmidt¹, Markus Dietlein¹, Alexander Drzezga¹

1 Department of Nuclear Medicine, University Hospital of Cologne, Cologne, Germany, **2** Institute of Radiochemistry and Experimental Molecular Imaging, University Hospital of Cologne, Cologne, Germany, **3** Institute of Neuroscience and Medicine–5 (Nuclear Chemistry), Research Center Jülich, Jülich, Germany

* jochen.hammes@uk-koeln.de



OPEN ACCESS

Citation: Hammes J, Hohberg M, Täger P, Wild M, Zlatopolskiy B, Krapf P, et al. (2018) Uptake in non-affected bone tissue does not differ between [¹⁸F]-DCFPyL and [⁶⁸Ga]-HBED-CC PSMA PET/CT. PLoS ONE 13(12): e0209613. <https://doi.org/10.1371/journal.pone.0209613>

Editor: Pradeep K. Garg, Biomedical Research Foundation, UNITED STATES

Received: August 23, 2018

Accepted: December 7, 2018

Published: December 20, 2018

Copyright: © 2018 Hammes et al. This is an open access article distributed under the terms of the [Creative Commons Attribution License](https://creativecommons.org/licenses/by/4.0/), which permits unrestricted use, distribution, and reproduction in any medium, provided the original author and source are credited.

Data Availability Statement: All numerical data analyzed in the study have been made publicly available under the URL <https://figshare.com/s/06cedad2c6a34650acb6>. With this dataset it is possible to replicate all analyses described in the manuscript. Furthermore, EBONI, the software we developed and applied to analyze the PSMA-PET/CT images, has been made publicly available under the URL https://github.com/jochenhammes/PSMA_Analysis/. According to EU-DSGVO, it is strictly prohibited to publish the full PET/CT imaging data, as it contains directly identifying

Abstract

Introduction

[⁶⁸Ga]PSMA-HBED-CC and [¹⁸F]DCFPyL show a high potential for the detection of recurrent prostate cancer. While ¹⁸F-based tracers have several advantages in availability and image resolution, their sensitivity in the skeleton might be impaired by released [¹⁸F]fluoride due to its high bone affinity. In turn, chemically unbound trivalent ⁶⁸Ga might also accumulate in osseous tissue, in cases of occupied binding sites of plasma proteins and thereby influence bone signal.

Methods

A comparison of average bone SUV was performed in 17 bone-negative and 4 bone-positive patients. All patients underwent PET/CT 125 minutes after application of [¹⁸F]DCFPyL and 73 minutes after application of [⁶⁸Ga]PSMA-HBED-CC at another date.

Results

Native SUVs in unaffected bone tissue and SUVs relative to liver uptake were lower in [¹⁸F]DCFPyL (0.49) than in [⁶⁸Ga]PSMA-HBED-CC scans (0.52). SUVs relative to gluteal muscles did not differ between the two tracers. Average lesional SUVs did not differ between tracers.

Conclusion

No difference of average bone signal intensity was observed for [¹⁸F]DCFPyL-PET/CT in comparison to [⁶⁸Ga]PSMA-HBED-CC scans indicating that diagnostic assessment of the skeleton is not affected by non-specific accumulation of free [¹⁸F]fluoride or ⁶⁸Ga.

information of the patients included in the study, e.g. full-body-anatomy including faces, etc. However, if comparable PET/CT datasets are available, this study can easily be replicated applying the above mentioned software package to it.

Funding: The authors received no specific funding for this work.

Competing interests: The authors have declared that no competing interests exist.

Introduction

Both ^{68}Ga - and ^{18}F -labeled tracers for imaging of prostate-specific membrane antigen (PSMA) such as [^{68}Ga]PSMA-HBED-CC and [^{18}F]DCFPyL have already demonstrated high potential for the detection of recurrent prostate cancer [1–4]. While ^{18}F -based tracers exhibit several advantages in terms of availability, production amount and image resolution, based on experiences with other ^{18}F based tracers, unspecific high tracer retention in bone tissue not affected by metastases might be responsible for a decrease of sensitivity in these areas due to defluorination. Although it has not been reported as a major limitation of this particular tracer before, it is conceivable that [^{18}F]fluoride released from [^{18}F]DCFPyL could cause a higher physiological background signal in osseous structures because it is a substrate of bone metabolism [5] and bone uptake has been traditionally used by other investigators as a measure of defluorination [6–8]. In turn, free trivalent ^{68}Ga that has dissolved from the chelating agent, might also have a high binding affinity to osseous structures, however this would require a state of occupied binding sites on plasma proteins or very low plasma transferrin levels [9]. In this study, we systematically compared the physiological tracer uptake in bone tissue in patients without osseous metastases who underwent both [^{68}Ga]PSMA-HBED-CC and [^{18}F]DCFPyL PET/CT using EBONI, a software tool to automatically quantify PET tracer uptake in bone tissue, published recently by us [10].

Methods

Compliance with ethical standards

All procedures performed in studies involving human participants were in accordance with the ethical standards of the institutional and/or national research committee and with the 1964 Helsinki declaration and its later amendments or comparable ethical standards. This article does not contain any studies with animals performed by any of the authors. The institutional review board of the University Hospital of Cologne has approved this study. Written informed consent was obtained from all individual participants included in the study.

21 patients underwent PSMA PET/CT with both [^{68}Ga]PSMA-HBED-CC and [^{18}F]DCFPyL in our department in a time frame of no longer than one month. Four of these patients were diagnosed with bone metastases. Average age of patients was 66.5 (+/- 8.5) years. Repeated PET/CTs with different PSMA-tracers were performed for clinical reasons (mostly due to a negative [^{68}Ga]PSMA-HBED-CC PET scan in patients with biochemical recurrence) as published previously [2, 3]. All PET/CT scans were performed on a Siemens Biograph mCT scanner (mCT 128 Flow Edge, Siemens, Knoxville, USA). PET/CT imaging was performed in accordance with the Institutional Review Board. Written informed consent was obtained from all individual participants included in the study. No change in therapeutic regimen had taken place between both scans. Acquisition and reconstruction (OSEM: 4 iterations, 12 subsets) was performed according to a protocol published previously [2]. In short, PET acquisition began 125 (+/- 12) minutes after injection of 311 (+/- 61) MBq [^{18}F]DCFPyL and 73 (+/- 14) minutes after injection of 162 (+/- 54) MBq [^{68}Ga]PSMA-HBED-CC. Average Radiochemical purity was well above 95% and did not differ significantly between tracers. For accurate determination of the activity of the radiopharmaceuticals the dose calibrator ISOMED 2010 (NUVIA Instruments GmbH, Dresden, Germany) was used. Quality control procedures of this class IIB medical device are carried out regularly according to DIN 6855–11.

The absence of bone metastases in 17 patients was confirmed by two experienced nuclear medicine physicians (PT, JH). Average standardized uptake value (SUV) in bone tissue (SUV_{bone}) in the bone negative group was determined automatically with EBONI. As previously

published, this software calculates tracer uptake selectively within bone tissue as defined by CT information based on Hounsfield-density [10]. The algorithmic function of EBONI is depicted in Fig 1. To avoid artefacts caused by spillover from unspecific uptake in extraosseous tissue, i.e. in facial bones due to uptake in the lacrimal and salivary glands [11], PET/CT datasets were analyzed starting from the upper thorax downwards. Average SUV in volumes of interest (VOIs) in the homogenous liver tissue (SUV_{liver}) as well as in the musculus gluteus maximus ($SUV_{gluteus}$) were extracted with VINCI (<http://vinci.sf.mpg.de>) [12]. VOIs were drawn

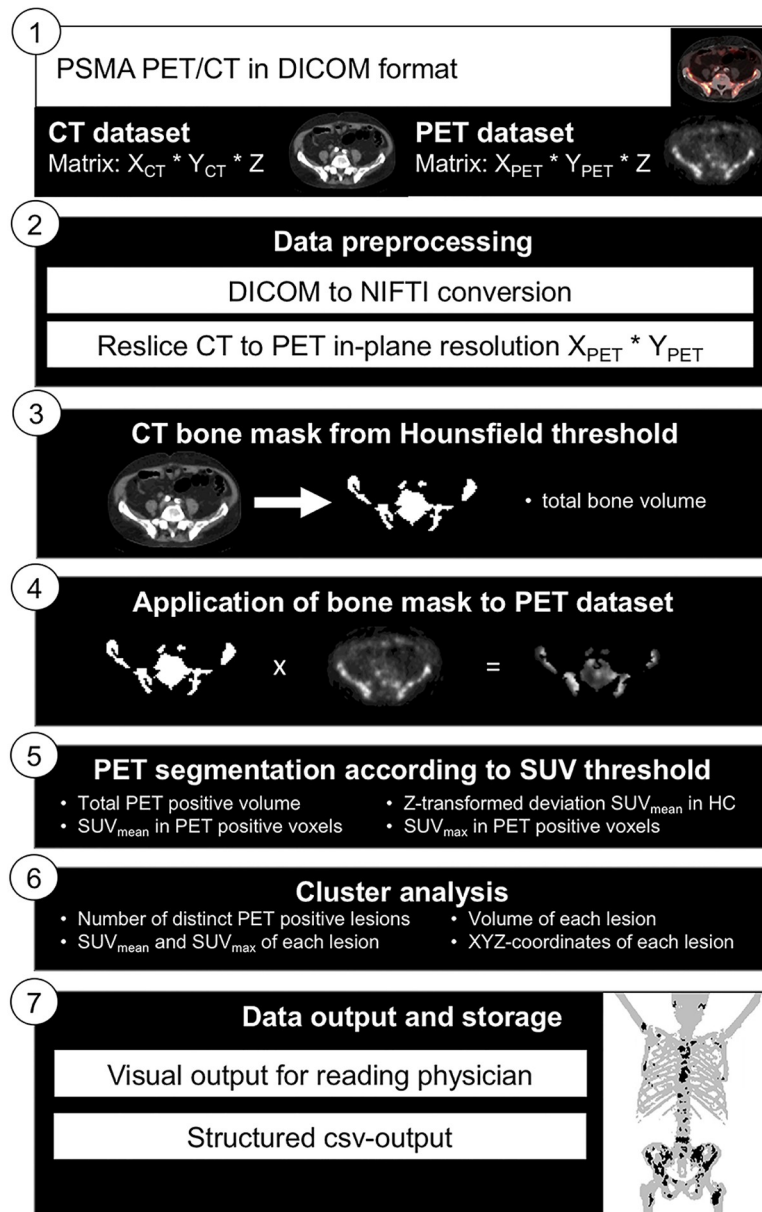


Fig 1. Algorithmic functionality of automated bone-VOI delineation and metastasis load quantification with EBONI in an exemplary patient with known osseous metastases of prostate cancer. csv = comma-separated values; HC = healthy controls. This figure was originally published in JNM [10]. Hammes et al. EBONI: A Tool for Automated Quantification of Bone Metastasis Load in PSMA PET/CT. *J Nucl Med.* 2018 Jul;59(7):1070–1075 by the Society of Nuclear Medicine and Molecular Imaging, Inc.

<https://doi.org/10.1371/journal.pone.0209613.g001>

manually so that they did not contain regions with elevated tracer uptake suspicious of being a metastasis. Minimum VOI volume was 5 ml. Exemplary VOIs are shown in Fig 2. Ratios between SUV_{bone} and individual $\text{SUV}_{\text{Liver}}$ and $\text{SUV}_{\text{gluteus}}$ were calculated. In the bone positive group, SUV_{max} and SUV_{mean} of the osseous metastases were determined by semiautomatic lesion segmentation in Siemens syngo.via (Lesion threshold 40% of SUV_{max}). Results were checked for normal distribution with Kolmogorov-Smirnov test and compared with Wilcoxon signed rank test. P values below 0.05 were considered significant. Fig 1 illustrates the algorithmic functionality of the creation of the bone-VOI with EBONI. Since we wanted to analyze tracer uptake in patients with no bone metastases, the CT-derived bone-VOI was applied without an SUV-threshold in step 4.

Results

Quantitative results with average SUV-values in the bone negative group are listed in Table 1 and displayed in Fig 3A. SUVs were not normally distributed. Unprocessed SUV_{bone} and SUV_{bone} relative to individual $\text{SUV}_{\text{liver}}$ was lower for [^{18}F]DCFPyL scans than for [^{68}Ga]PSMA-HBED-CC scans. SUV_{bone} relative to individual $\text{SUV}_{\text{gluteus}}$ did not differ between [^{18}F]DCFPyL and [^{68}Ga]PSMA-HBED-CC. Radiochemical purity was 95.5% for [^{18}F]DCFPyL and 98.9% for [^{68}Ga]PSMA-HBED-CC but did not differ significantly

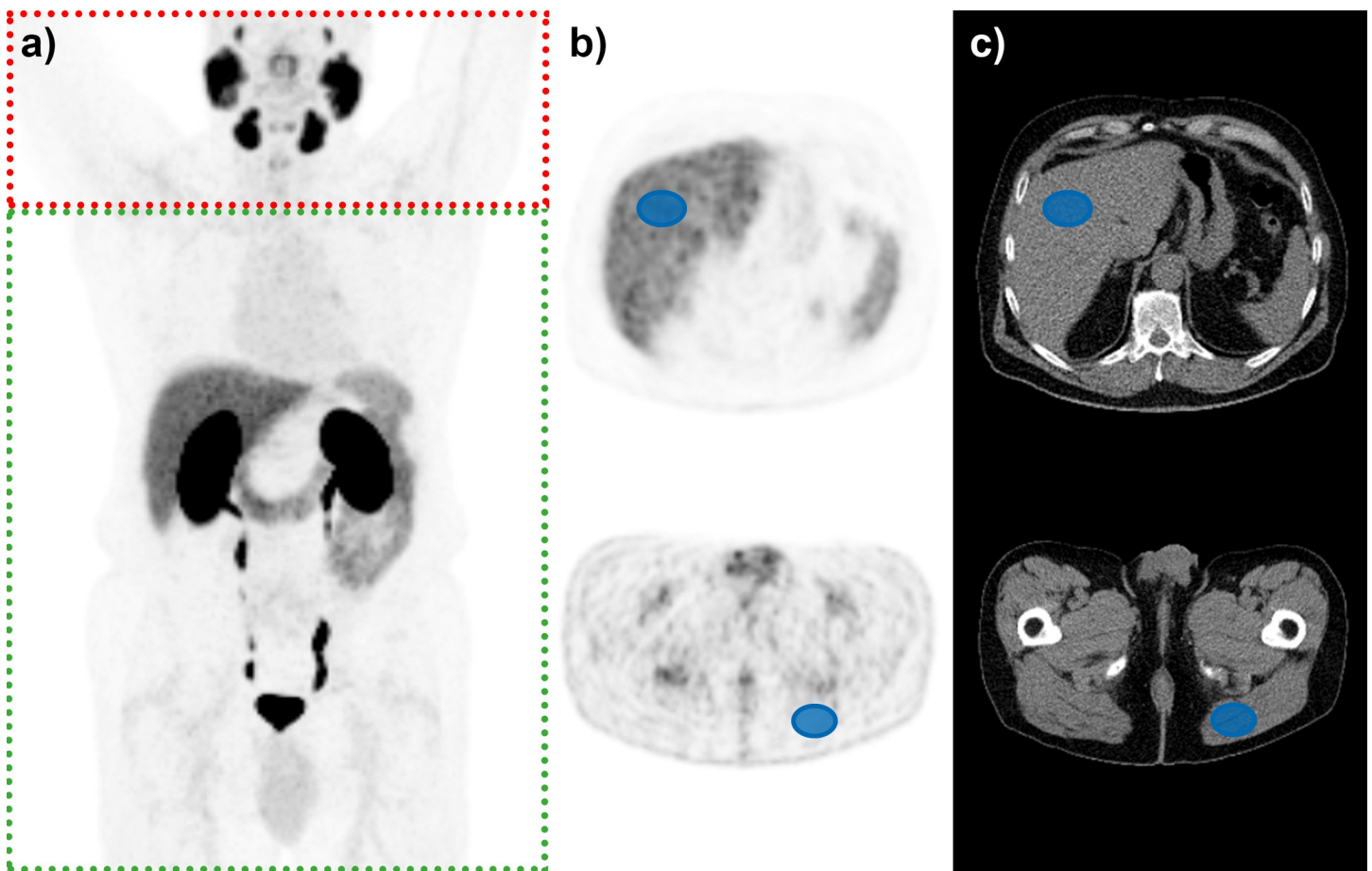


Fig 2. Exemplary PET dataset (a) and placement of VOIs (b,c). Red-dotted area was excluded from the analysis to avoid spillover into bone voxels caused by uptake in salivary and lacrimal glands.

<https://doi.org/10.1371/journal.pone.0209613.g002>

Table 1. Quantitative results in bone negative group. Average values and standard deviation.

	¹⁸ F-DCFPyL	⁶⁸ Ga-PSMA-HBED-CC	p (Wilcoxon)
SUV _{liver}	6.1 (1.2)	4.6 (1.0)	<0.01*
SUV _{gluteus}	0.35 (0.13)	0.36 (0.08)	0.62
SUV _{bone}	0.49 (0.08)	0.52 (0.06)	0.03*
SUV _{bone} /SUV _{liver}	0.082 (0.02)	0.117 (0.019)	<0.01*
SUV _{bone} /SUV _{gluteus}	1.50 (0.37)	1.54 (0.39)	0.55

* indicates statistical significance

<https://doi.org/10.1371/journal.pone.0209613.t001>

(p = 0.07). Average SUV_{max} and SUV_{mean} of bone metastases in the bone positive group are listed in Table 2 and Fig 3B. Average SUVs in bone metastases and SUVs relative to the gluteal reference region were numerically higher in the [¹⁸F]DCFPyL scans, although the difference did not exceed the significance threshold.

Discussion

Here, we demonstrate that average SUV of [¹⁸F]DCFPyL and [⁶⁸Ga]PSMA-HBED-CC in bone tissue (unaffected by metastases of prostate cancer) is comparable between tracers. Our data leads to the conclusion, that, for these PSMA-tracers, chemically unbound radionuclides apparently only occur in quantities that are small enough not to affect the intensity of the background signal in bone tissue. To date, both tracer families are considered widely interchangeable for most clinical applications [13], while there is evidence that the average SUV of PSMA positive lesions is higher for [¹⁸F]DCFPyL than for [⁶⁸Ga]PSMA-HBED-CC (when acquired according to the mentioned protocols), as reported earlier by our group [2]. Here, we could not confirm a significant difference of lesional SUVs between the tracers, however, we attribute this fact to the small number of bone-positive patients we had available to include in this study.

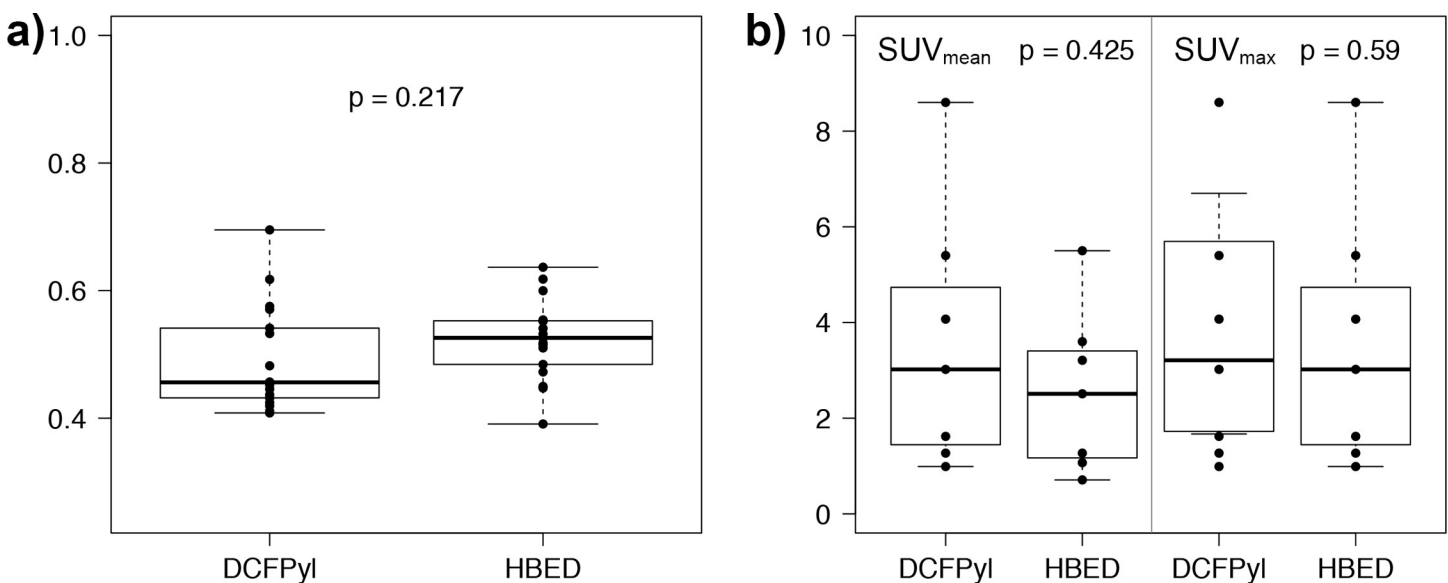


Fig 3. a) Average SUVs in unaffected bone tissue in 17 patients without bone metastases. **b)** SUV_{mean} and SUV_{max} in a total of seven bone metastases in the group of patients with bone metastases.

<https://doi.org/10.1371/journal.pone.0209613.g003>

Table 2. Quantitative results in bone metastases.

	DCFpyL	HBED	p
Bone metastasis SUV _{max}	4,56 (3,86)	3,57 (2,74)	0,113
SUV _{mean}	3,54 (2,78)	2,55 (1,71)	0,092
SUV _{liver}	6,81 (1,38)	5,38 (0,5)	0,080
SUV _{gluteus}	0,35 (0,07)	0,36 (0,04)	0,869
SUV _{max} / SUV _{liver}	0,64 (0,45)	0,69 (0,56)	0,588
SUV _{mean} / SUV _{liver}	0,5 (0,33)	0,49 (0,35)	0,891
SUV _{max} / SUV _{gluteus}	12,69 (9,44)	10,79 (9,53)	0,189
SUV _{mean} / SUV _{gluteus}	9,9 (6,86)	7,62 (5,92)	0,062

<https://doi.org/10.1371/journal.pone.0209613.t002>

It needs to be taken into account that the imaging protocols were not entirely comparable for the two tracers. Although the same scanner was used for acquisition of all images, as compared to [⁶⁸Ga]PSMA-HBED-CC, a higher dose of [¹⁸F]DCFpyL has been injected and the images were acquired significantly later, which corresponds to the usual procedure for this tracer. The [¹⁸F]DCFpyL tracer's higher half-life and production yield enable this approach, which has been chosen because a better lesion contrast and resulting higher sensitivity can be expected [2, 3].

We believe that these differences in the acquisition protocols should not have considerably affected the results of this study. First, it appears reasonable to compare the two tracers according to the usual conditions of their use in everyday practice. Second, we would not expect that later image acquisition or injection of higher tracer doses would lead to a decrease in relative bone uptake of the tracer.

The level of skeletal binding depends on the radiochemical purity achieved during tracer production. In our sample, the radiochemical purities of both tracers did not differ significantly. This further stresses the understanding that skeletal signal is only marginally affected by unbound ¹⁸F-fluoride and does not lead to differences in image quality. In addition to this observation, considering the typical biological distribution of free Gallium, an affection of the bone signal due to unspecific accumulation of the nuclide released from [⁶⁸Ga]PSMA-HBED-CC could only be expected, if the Gallium binding sites of peripheral plasma proteins were occupied or plasma protein concentrations were unusually low. Therefore, under normal circumstances, an influence of free ⁶⁸Ga could only be expected if it was administered in amounts that are several orders of magnitude higher than those typically administered in human PET examinations [9].

The aforementioned advantages of [¹⁸F]DCFpyL together with the findings of this study support the notion that the ¹⁸F-labeled tracer [¹⁸F]DCFpyL may be advantageous for clinical routine application. These findings, however, cannot be generalized to other ¹⁸F-labeled PSMA-tracers like [¹⁸F]PSMA-1007 [14] with different in vivo characteristics and therefore will have to be evaluated accordingly.

Author Contributions

Conceptualization: Melanie Hohberg, Bernd Neumaier, Markus Dietlein, Alexander Drzezga.

Data curation: Jochen Hammes, Melanie Hohberg, Markus Dietlein.

Formal analysis: Jochen Hammes, Philipp Täger.

Funding acquisition: Alexander Drzezga.

Investigation: Jochen Hammes.

Methodology: Jochen Hammes, Melanie Hohberg, Philipp Täger.

Project administration: Jochen Hammes.

Resources: Markus Wild, Boris Zlatopolskiy, Philipp Krapf, Bernd Neumaier, Klaus Schomäcker, Markus Dietlein.

Software: Jochen Hammes.

Supervision: Carsten Kobe, Matthias Schmidt.

Validation: Markus Wild, Bernd Neumaier, Klaus Schomäcker, Carsten Kobe, Alexander Drzezga.

Visualization: Jochen Hammes.

Writing – original draft: Jochen Hammes.

Writing – review & editing: Melanie Hohberg, Philipp Täger, Markus Wild, Boris Zlatopolskiy, Philipp Krapf, Bernd Neumaier, Klaus Schomäcker, Carsten Kobe, Matthias Schmidt, Markus Dietlein, Alexander Drzezga.

References

1. Eiber M, Maurer T, Souvatzoglou M, Beer AJ, Ruffani A, Haller B, et al. Evaluation of Hybrid ⁶⁸Ga-PSMA Ligand PET/CT in 248 Patients with Biochemical Recurrence After Radical Prostatectomy. *J Nucl Med* 2015; 56: 668–674. <https://doi.org/10.2967/jnumed.115.154153> PMID: 25791990
2. Dietlein M, Kobe C, Kuhnert G, Stockter S, Fischer T, Schomäcker K, et al. Comparison of [(18F)] DCFPyL and [(68)Ga]Ga-PSMA-HBED-CC for PSMA-PET imaging in patients with relapsed prostate cancer. *Mol Imaging Biol* 2015; 17: 575–584. <https://doi.org/10.1007/s11307-015-0866-0> PMID: 26013479
3. Dietlein F, Kobe C, Neubauer S, Schmidt M, Stockter S, Fischer T, et al. PSA-Stratified Performance of 18F- and 68Ga-PSMA PET in Patients with Biochemical Recurrence of Prostate Cancer. *J Nucl Med* 2017; 58: 947–952. <https://doi.org/10.2967/jnumed.116.185538> PMID: 27908968
4. Rowe SP, Macura KJ, Mena E, Blackford AL, Nadal R, Antonarakis ES, et al. PSMA-Based [18F] DCFPyL PET/CT Is Superior to Conventional Imaging for Lesion Detection in Patients with Metastatic Prostate Cancer. *Mol Imaging Biol* 2016; 18: 411–419. <https://doi.org/10.1007/s11307-016-0957-6> PMID: 27080322
5. Fonager RF, Zacho HD, Langkilde NC, Fledelius J, Ejlersen JA, Hendel HW, et al. Prospective comparative study of 18F-sodium fluoride PET/CT and planar bone scintigraphy for treatment response assessment of bone metastases in patients with prostate cancer. *Acta Oncol* 2018; 0: 1–7.
6. Jahan M, Eriksson O, Johnström P, Korsgren O, Sundin A, Johansson L, et al. Decreased defluorination using the novel beta-cell imaging agent [18F]JFE-DTBZ-d4 in pigs examined by PET. *EJNMMI Res* 2011; 1: 33. <https://doi.org/10.1186/2191-219X-1-33> PMID: 22214308
7. Ponde DE, Dence CS, Oyama N, Kim J, Tai Y, Laforest R, et al. 18F-Fluoroacetate: A Potential Acetate Analog for Prostate Tumor Imaging—In Vivo Evaluation of 18F-Fluoroacetate Versus 11C-Acetate. *J Nucl Med* 2007; 48: 420–428. PMID: 17332620
8. Tipre DN, Zoghbi SS, Liow J-S, Green MV, Seidel J, Ichsie M, et al. PET Imaging of Brain 5-HT1A Receptors in Rat In Vivo with 18F-FCWAY and Improvement by Successful Inhibition of Radioligand Defluorination with Miconazole. *J Nucl Med* 2006; 47: 345–353. PMID: 16455642
9. Hayes RL. The interaction of gallium with biological systems. *Int J Nucl Med Biol* 1983; 10: 257–261. PMID: 6363324
10. Hammes J, Täger P, Drzezga A. EBONI: A tool for automated quantification of bone metastasis load in PSMA PET/CT. *J Nucl Med*. 2018 Jul; 59(7):1070–1075. <https://doi.org/10.2967/jnumed.117.203265> PMID: 29242401
11. Hohberg M, Eschner W, Schmidt M, Dietlein M, Kobe C, Fischer T, et al. Lacrimal Glands May Represent Organs at Risk for Radionuclide Therapy of Prostate Cancer with [(177)Lu]DKFZ-PSMA-617. *Mol Imaging Biol MIB* 2016; 18: 437–445. <https://doi.org/10.1007/s11307-016-0942-0> PMID: 26920354
12. Vollmar S, Čížek J, Sué M, Klein J, Jacobs A, Herholz K. VINCI -Volume Imaging in Neurological Research, Co-Registration and ROIs included. In: *Forschung und wissenschaftliches Rechnen 2003* (Kremer K, Macho V, eds). Göttingen: GWDG, 2004, pp. 115–131.

13. Kesch C, Kratochwil C, Mier W, Kopka K, Giesel FL. 68Ga or 18F for Prostate Cancer Imaging? *J Nucl Med* 2017; 58: 687–688. <https://doi.org/10.2967/jnumed.117.190157> PMID: 28408526
14. Giesel FL, Hadaschik B, Cardinale J, Radtke J, Vinsensia M, Lehnert W, et al. F-18 labelled PSMA-1007: biodistribution, radiation dosimetry and histopathological validation of tumor lesions in prostate cancer patients. *Eur J Nucl Med Mol Imaging* 2017; 44: 678. <https://doi.org/10.1007/s00259-016-3573-4> PMID: 27889802